# QM/MM Study of Thymidylate Synthase: Enzymatic Motions and the Temperature Dependence of the Rate Limiting Step[†]

**Natalia Kanaan, Sergio Martí,\* and Vicent Moliner\***

*Departament de Química Física i Analítica, Universitat Jaume I, 12071 Castellón, Spain*

**Amnon Kohen**

*Department of Chemistry, University of Iowa, Iowa City, Iowa 52242*

Thymidylate synthase (TS) is an enzyme that catalyzes a complex cascade of reactions. A theoretical study of the reduction of an exocyclic methylene intermediate by hydride transfer from the 6S position of 5,6,7,8-tetrahydrofolate (H$_4$folate), to form 2′-deoxyuridine 5′-monophosphate (dTMP) and 7,8-dihydrofolate (H$_2$folate), has been carried out using hybrid quantum mechanics/molecular mechanics methods. This step is of special interest because it is the rate-limiting step of the reaction catalyzed by TS. The acceptor of this hydride is an intermediate that is covalently bound to the enzyme via a thioether bond to an overall conserved active site cysteine residue (Cys146 in *Escherichia coli*). Heretofore, whether the hydride transfer precedes the thiol abstraction that releases the product from the enzyme or whether these two processes are concerted has been an open question. We have examined this step in terms of free energy surfaces obtained at the same temperatures we previously used in experimental studies of this mechanistic step (273–313 K). Analysis of the results reveals that substantial features of the reaction and the nature of the H-transfer seem to be temperature independent, in agreement with our experimental data. The findings also indicate that the hydride transfer and the scission of Cys146 take place in a concerted but asynchronous fashion. This 1,3-S$_N$2 substitution is assisted by arginine 166 and several other arginine residues in the active site that polarize the carbon–sulfur bond and stabilize the charge transferred from cofactor to substrate. Finally, the simulation elucidates the molecular details of the enzyme's motion that brings the system to its transition state and, in accordance with the experimental data, indicates that this "tunneling ready" conformation is temperature independent.

## Introduction

Thymidylate synthase (TS, EC 2.1.1.45) catalyzes the reductive methylation of 2′-deoxyuridine 5′-monophosphate (dUMP) to 2′-deoxythymidine 5′-monophosphate (dTMP) using the cofactor N5,N10-methylene-5,6,7,8-tetrahydrofolate (CH$_2$H$_4$folate) as a donor of both methylene and hydride, and producing 7,8-dihydrofolate (H$_2$ folate). The overall reaction is depicted in Scheme 1.

This enzyme is crucial for DNA biosynthesis, as it forms one of its building blocks (thymidine). Consequently, it is an anticancer and antibiotic drug target, and great interest has been shown for many years in the details of its catalytic activity. A better understanding of its molecular mechanism may lead to more specific drugs that would specifically inhibit TS activity in cancerous or bacterial cells but not in normal human cells.

We have recently studied the entire TS multistep mechanism Scheme 2 by means of hybrid quantum mechanics/molecular mechanics (QM/MM) potential energy surfaces exploration.[1] These calculations indicated that hydride transfer from the 6S position of H$_4$folate, forming dTMP and H$_2$folate (step 5 in Scheme 2), is the rate determining step of the overall reaction. This finding was in good agreement with our experimental findings.[2] Because the hydride transfer is rate limiting and practically not reversible, processes that are concerted or those that follow this step are not experimentally accessible. Consequently, heretofore, the lack of such experimental information

**SCHEME 1: Overall Reaction Catalyzed by TS (R = 2′-Deoxyribose 5′-phosphate and R′ = *p*-Aminobenzoylglutamate)**
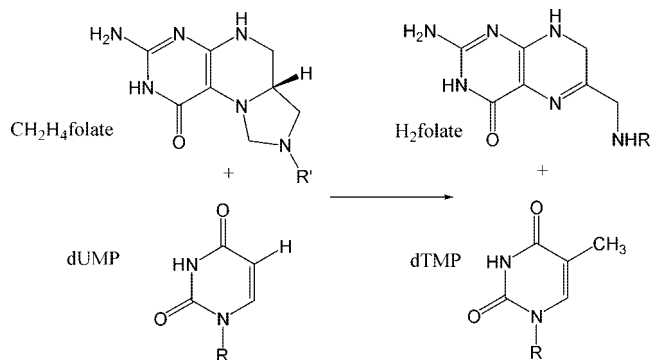


prohibited the elucidation of the relations between the H-transfer and the dissociation of the thioester bond that leads to the release of the product from the enzyme.[3]

As illustrated in Scheme 3, two possible mechanisms would be consistent with the chemical transformation of this rate limiting step: (A) the hydride transfer and the thiol abstraction taking place in a concerted way, which can be viewed as a 1,3-S$_N$2 substitution, and (B) the hydride transfer from C6 of H$_4$folate to C7 of the exocyclic methylene preceding the elimination of the thioether from C6 of dUMP (i.e., the intermediate anion could be stabilized by enzymatic protonation of the C4 carbonyl, as proposed for the initial Michael addition,

**SCHEME 2: Minimal Reaction Mechanism of TS (R = 2′-Deoxyribose-5′-phosphate and R′ = *p*-Aminobenzoylglutamate)**
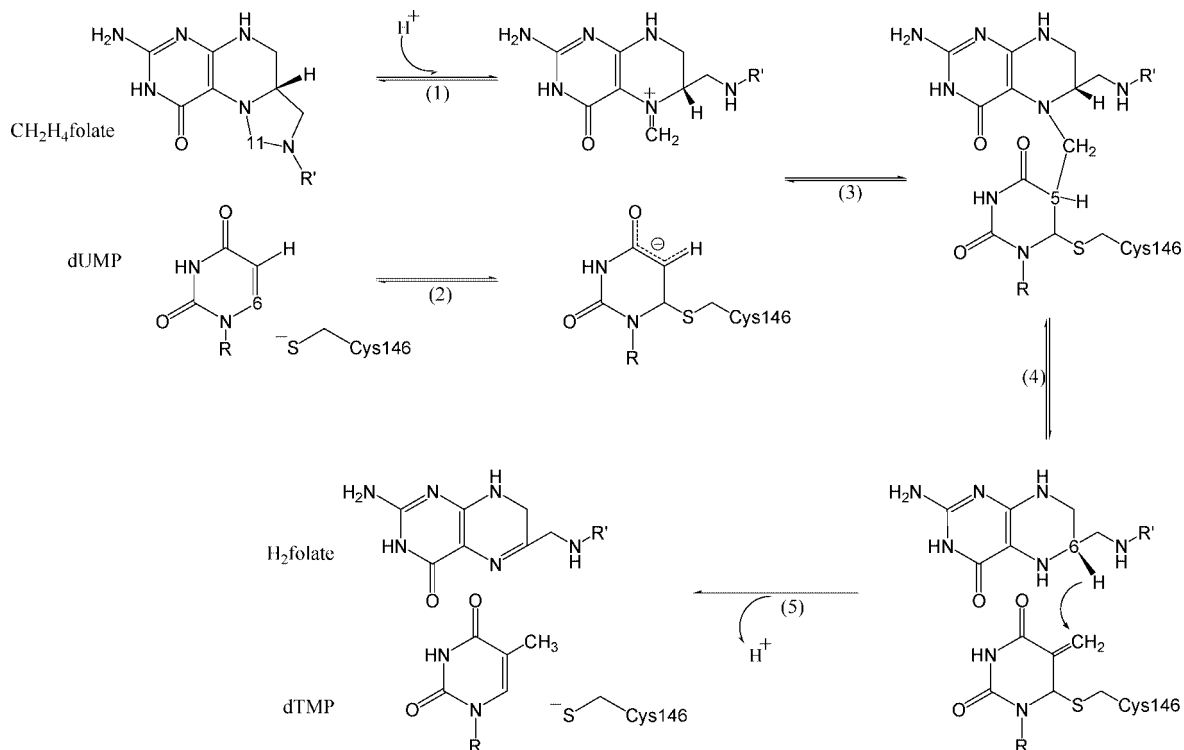


**SCHEME 3: Rate Limiting Step of the Reaction Catalyzed by TS[a]**
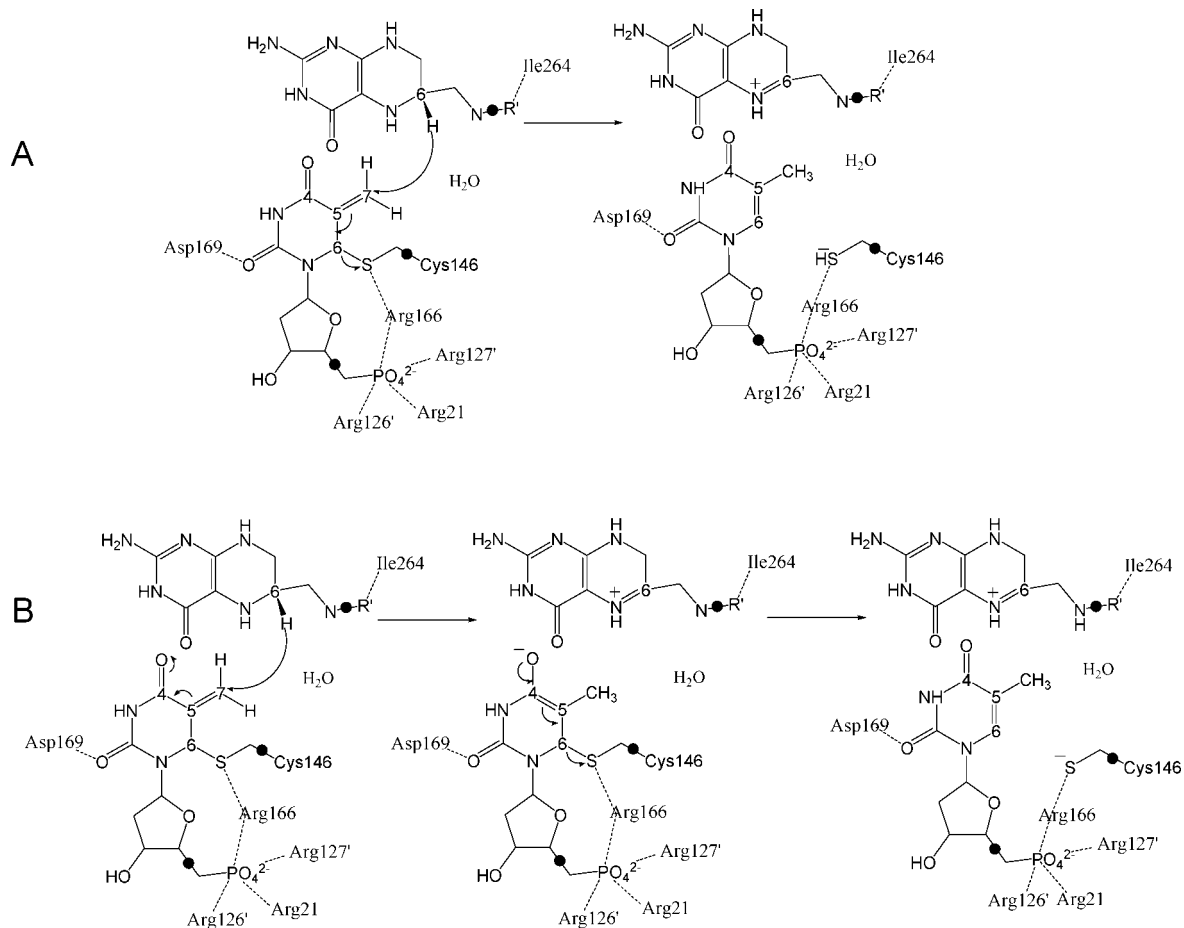


[a] Two possible mechanisms are depicted: A, concerted mechanism; B, stepwise mechanism. The link atoms between the QM and the MM regions are indicated as •.

step 2, Scheme 2). Calculations that examine the nature of this step are not limited by the lack of reversibility and may provide the long sought insight regarding the nature of this TS-unique chemistry.

The current study examined this rate-limiting hydride transfer using two-dimensional potential of mean force (PMF) calculations carried out at the same four temperatures used in the experimental study.[2] In particular, the antisymmetric combination of the distances describing the breaking and forming bonds on the hydride transfer step ($d_{CH} - d_{HC}$) and the distance between the C6 of the dUMP and the sulfur of the Cys146 ($d_{CS}$) have been used as distinguished reaction coordinates. The results shed light on the nature and the molecular details of the reaction, as well as on the role of the enzyme's dynamics and active site residues in catalysis.

**Computational Methods.** The initial geometry for carrying out the calculations was the X-ray crystal structure of a ternary complex of *Escherichia coli* TS with dUMP and an antifolate, 10-propargyl-5,8-dideazafolate (CB3717), PDB ID 2TSC.[4−6] The inhibitor was replaced by the cofactor structure and the hydrogen atoms were incorporated into the structure using DYNAMO.[7] After that, the "cluster method",[8] as implemented by Field and co-workers,[9] was used to recalculate the standard p$K_a$ values of the titratable amino acids of the enzyme.

The total charge of the system was not neutral, and 24 sodium counterions were placed in optimal electrostatic positions around the enzyme, further than 10.5 Å from any atom of the system or 5 Å from another sodium, using a regular grid of 0.5 Å. The system was then placed in a prerelaxed orthorhombic box of water molecules (80 Å × 80 Å × 100 Å). All the water molecules with an oxygen atom closer than 2.8 Å to any heavy atom were removed.

The system was divided into a QM region, which includes the pteridine ring of the folate, the six-membered ring, and the ribose ring of the dUMP, part of the Cys146 and a crystallization water molecule, comprising 57 atoms (Scheme 3). The MM region involves the rest of the active site, the enzyme, the crystallization and solvation water molecules and the counterions.

The AM1[10] semiempirical Hamiltonian was chosen to describe the QM part and OPLS-AA[11] and TIP3P[12] force fields were chosen for the MM region. To satisfy the valence of the QM fragments when the QM-MM boundary divides a covalent bond, the link atom method was used[13,14] (marked by • in Scheme 3). The nonbonding interactions were treated by periodic boundary conditions, using a switch function with a cutoff distance in the range 16−18 Å. Then, the system was relaxed by means of hybrid QM/MM molecular dynamics (MD). A Langevin bath (293 K) was used, in a canonical thermodynamic ensemble (NVT). The MD was run for 200 ps with an integration step size of 1 fs.

Two dimensional PMF (2D-PMF) at four different temperatures (278, 293, 303, and 313 K) were obtained using the weighted histogram analysis method (WHAM) combined with the umbrella sampling approach[15,16] as implemented in DYNAMO. The distinguished reaction coordinates were the antisymmetric combination of the distances describing the breaking and forming bonds on the hydride transfer step ($d_{CH} - d_{HC}$) and the distance between the C6 of the dUMP and the sulfur atom of the Cys146 ($d_{CS}$). A total of 61 simulations were performed at different values of $d_{CH} - d_{HC}$ (61 simulations in a range from −1.5 to +1.5 Å), with an umbrella force constant of 2500 kJ·mol$^{-1}$·A$^{-1}$ for each particular value of the distance $d_{CS}$ (28 simulations with a force constant of 2500 kJ·mol$^{-1}$·A$^{-1}$, from 1.8 to 4.5 Å). Consequently, there are 1708 windows per PMF.

The values of the variables sampled during the simulations were then pieced together to construct a full distribution function from which the 2D-PMF was obtained. On each window, 5 ps of relaxation was followed by 10 ps of production with a time step of 0.5 ps due to the nature of the chemical step involving a hydrogen transfer. The starting point for the four PMF-2Ds was the pre-equilibrated transition structure at 293 K, within an averaged rmsd (root-mean-square deviation) of the temperature for all the windows at each temperature never higher than 2.6 K (this value corresponds to the 313 K surface). Thus, the low differences in temperature (at most 20 K) have been in all cases successfully overcome with the short relaxation dynamics, confirming the enzyme was equilibrated at the new temperature. The Verlet algorithm was used to update the velocities.

A note of caution has to be introduced at this point because two-dimensional free energy surfaces, as the 2D-PMF computed in this study, are associated to two coordinates, and not to only one, $\xi_0$, as defined in eq 1.

$$\text{PMF}(\xi_0) = -\frac{1}{\beta} \ln \int \delta(\xi(r) - \xi_0) e^{-\beta U(r)} \, dr \quad (1)$$

As a consequence, the energy should be integrated over the additional coordinate, $\gamma$, as defined in eq 2.

$$\text{PMF}(\xi_0) = -\frac{1}{\beta} \ln \int e^{-\beta \text{PMF}(\xi_0, \gamma_0)} \, d\gamma \quad (2)$$

Nevertheless, because this error is not significant and, in any case, similar for all the four free energy surfaces computed in this study, comparison of free energy barriers can be properly estimated without integration over additional variables.

## Results

As mentioned above, four 2D-PMFs were obtained at four different temperatures (278, 293, 303 and 313 K), which are the same temperatures we examined experimentally,[2] and the results are shown in Figure 1. The first conclusion that can be derived from Figure 1 is that the topology of the free energy surfaces is almost independent of the temperature. This would imply temperature independent kinetic isotope effects (KIEs) in accordance with the experimental findings.[2] All free energy surfaces describe a concerted but asynchronous step, with a transition state quadratic region located in a very early stage of the C−S breaking bond process, whereas hydride transfer is between the donor and acceptor atoms. Additionally, the calculated activation free energy, $\Delta G^{\ddagger}$, is in the 22−24 kcal·mol$^{-1}$ range (22.2, 23.3, 24,4 and 24.1 kcal·mol$^{-1}$ for the four different temperatures, respectively). These values are slightly smaller than the potential energy barrier, 26 kcal·mol$^{-1}$, previously reported by us.[1] These results are consistent with a small and positive entropy of activation.

In pursuit of a molecular insight into the source of the observed temperature independent KIEs, of this hydride transfer step,[2] averaged values of key geometrical parameters of structures selected from reactant state, transition state, and product state have been obtained at the four different temperatures. The results are listed in Tables 1 and 2.

The first conclusion that can be derived from the results presented in Table 1 is the invariance of the location of the saddle point on the free energy surfaces. The distinguished reaction coordinates (the antisymmetric combination of distances describing the hydride transfer and the interatomic C6−S distance) are close to −0.06 and +2.02 Å, respectively, at all temperatures. This indicates that in all transition state structures, the transferring hydrogen is between donor and acceptor atoms,
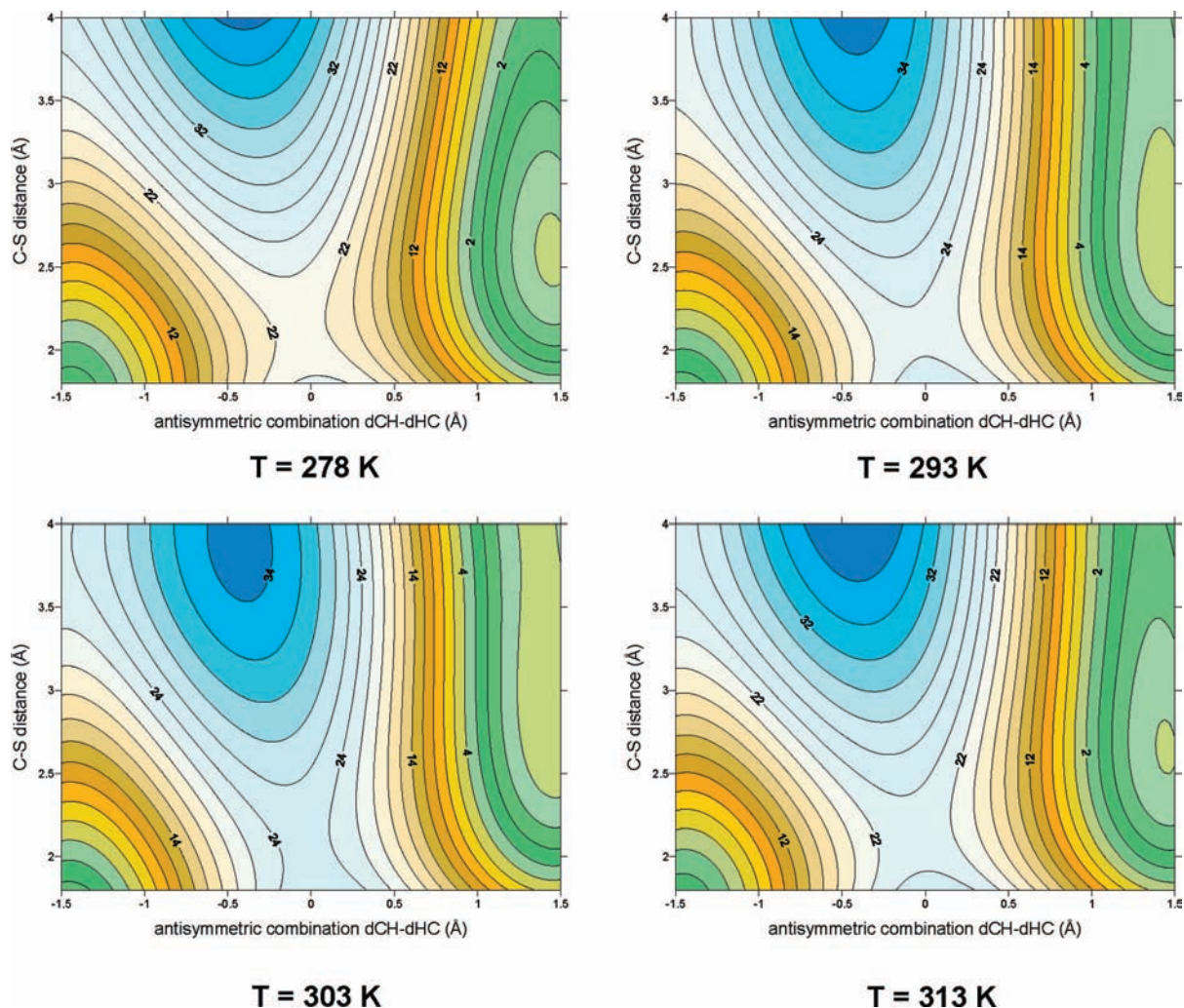
QM/MM Study of Thymidylate Synthase

*J. Phys. Chem. A, Vol. 113, No. 10, 2009* **2179**



**Figure 1.** Two-dimensional PMF performed at four different temperatures: 278, 293, 303, and 313 K. The distinguished reaction coodinates are C6(dUMP)−S(Cys146) and the antisymmetric combination of the breaking and forming bonds of the transferred hydrogen atom, dCH−dHC (in Å). Values on isoenergetic lines are reported in kcal·mol$^{-1}$.

**TABLE 1: Key Averaged Distances (Å) Related to the Substrate and Cofactor, Obtained at the Reactant, Transition, and Product States of the Rate Limiting Hydride Transfer Step of the TS Catalyzed Reaction, Computed at the AM1/MM Level, at the Four Different Temperatures 278, 293, 303, and 313 K**

| $T$/K | interatomic distances[a] | reactant state | transition state | product state |
|---|---|---|---|---|
| 278 | C6(FOL)−H6(FOL) | $1.14 \pm 0.03$ | $1.34 \pm 0.04$ | $4.2 \pm 0.6$ |
| | H6(FOL)−C7(UMP) | $2.80 \pm 0.20$ | $1.42 \pm 0.04$ | $1.12 \pm 0.03$ |
| | antisymmetric combination | $-1.66 \pm 0.20$ | $-0.08 \pm 0.03$ | $3.1 \pm 0.6$ |
| | C6(FOL)−C7(UMP) | $3.50 \pm 0.18$ | $2.74 \pm 0.06$ | $4.2 \pm 0.3$ |
| | C6(UMP)−S(Cys146) | $1.98 \pm 0.05$ | $2.00 \pm 0.06$ | $3.2 \pm 0.3$ |
| 293 | C6(FOL)−H6(FOL) | $1.14 \pm 0.03$ | $1.35 \pm 0.04$ | $4.3 \pm 0.8$ |
| | H6(FOL)−C7 (UMP) | $3.03 \pm 0.21$ | $1.41 \pm 0.04$ | $1.12 \pm 0.03$ |
| | antisymmetric combination | $-1.89 \pm 0.21$ | $-0.06 \pm 0.04$ | $3.2 \pm 0.8$ |
| | C6(FOL)−C7 (UMP) | $3.60 \pm 0.21$ | $2.73 \pm 0.07$ | $4.0 \pm 0.3$ |
| | C6(UMP)−S(Cys146) | $1.97 \pm 0.05$ | $2.02 \pm 0.07$ | $3.1 \pm 0.3$ |
| 303 | C6(FOL)−H6(FOL) | $1.14 \pm 0.03$ | $1.36 \pm 0.04$ | $4.4 \pm 0.9$ |
| | H6(FOL)−C7(UMP) | $2.75 \pm 0.21$ | $1.40 \pm 0.04$ | $1.12 \pm 0.03$ |
| | antisymmetric combination | $-1.61 \pm 0.22$ | $-0.04 \pm 0.04$ | $3.3 \pm 0.9$ |
| | C6(FOL)−C7(UMP) | $3.49 \pm 0.21$ | $2.74 \pm 0.07$ | $4.1 \pm 0.3$ |
| | C6(UMP)−S(Cys146) | $1.97 \pm 0.05$ | $2.04 \pm 0.08$ | $3.2 \pm 0.3$ |
| 313 | C6(FOL)−H6(FOL) | $1.14 \pm 0.03$ | $1.36 \pm 0.04$ | $4.3 \pm 0.8$ |
| | H6(FOL)−C7(UMP) | $2.92 \pm 0.24$ | $1.41 \pm 0.04$ | $1.12 \pm 0.03$ |
| | antisymmetric combination | $-1.8 \pm 0.3$ | $-0.05 \pm 0.04$ | $3.17 \pm 0.8$ |
| | C6(FOL)−C7(UMP) | $3.43 \pm 0.19$ | $2.74 \pm 0.07$ | $4.0 \pm 0.3$ |
| | C6(UMP)−S(Cys146) | $1.97 \pm 0.06$ | $2.02 \pm 0.07$ | $3.1 \pm 0.3$ |

[a] FOL indicates an atom on the folate derivative and UMP indicates an atom on the thymine derivative.

whereas the carbon sulfur breaking bond process, defined by the C6(UMP)−S(Cys146) distance, is in an early stage of the reaction. This last bond is completely broken in products at all temperatures ($3.15 \pm 0.03$ Å). These results are in accordance

**TABLE 2: Key Substrate−Protein Averaged Distances (in Å) Obtained at the Reactant, Transition, and Product States of the Hydride Transfer Step of the TS Catalyzed Reaction, Computed at the AM1/MM Level, at the Four Different Temperatures 278, 293, 303, and 313 K[a]**

Reactant State

| | | | | | | T/K | | |
| --- | --- | --- | --- | --- | --- | --- | --- | --- |
| | | | | | 278 | 293 | 303 | 313 |
| CYS146 | S | WAT | 40 | H2 | 1.93 ± 0.12 | 1.94 ± 0.13 | 1.94 ± 0.13 | 1.94 ± 0.13 |
| CYS146 | S | ARG | 166 | HH11 | 2.4 ± 0.3 | 2.5 ± 0.3 | 2.5 ± 0.3 | 2.6 ± 0.3 |
| UMP | O2 | ASP | 169 | H | 2.00 ± 0.11 | 2.10 ± 0.15 | 2.03 ± 0.11 | 1.98 ± 0.11 |
| UMP | P | ARG | 166 | HH22 | 2.32 ± 0.10 | 2.33 ± 0.09 | 2.31 ± 0.09 | 2.35 ± 0.10 |
| UMP | O1P | ARG′ | 126 | HH12 | 2.08 ± 0.20 | 2.17 ± 0.20 | 2.25 ± 0.19 | 2.10 ± 0.22 |
| UMP | O1P | ARG | 21 | HE | 1.59 ± 0.09 | 1.61 ± 0.10 | 1.62 ± 0.10 | 1.68 ± 0.13 |
| UMP | O2P | ARG′ | 126 | HE | 1.72 ± 0.12 | 1.69 ± 0.12 | 1.70 ± 0.12 | 1.69 ± 0.12 |
| UMP | O2P | ARG | 166 | HH22 | 1.63 ± 0.11 | 1.63 ± 0.12 | 1.63 ± 0.13 | 1.62 ± 0.12 |
| UMP | O3P | ARG | 166 | HH12 | 1.75 ± 0.15 | 1.77 ± 0.17 | 1.78 ± 0.16 | 1.77 ± 0.19 |
| UMP | O3P | ARG | 166 | HH22 | 2.37 ± 0.18 | 2.37 ± 0.18 | 2.35 ± 0.19 | 2.42 ± 0.19 |
| UMP | O3P | ARG′ | 127 | HH11 | 1.67 ± 0.11 | 1.64 ± 0.12 | 1.66 ± 0.12 | 1.67 ± 0.13 |

Transition State

| | | | | | | T/K | | |
| --- | --- | --- | --- | --- | --- | --- | --- | --- |
| | | | | | 278 | 293 | 303 | 313 |
| CYS146 | S | WAT | 40 | H2 | 1.93 ± 0.12 | 1.92 ± 0.12 | 1.91 ± 0.12 | 1.92 ± 0.13 |
| CYS146 | S | ARG | 166 | HH11 | 2.4 ± 0.3 | 2.4 ± 0.3 | 2.3 ± 0.3 | 2.4 ± 0.3 |
| UMP | O2 | ASP | 169 | H | 1.97 ± 0.11 | 2.02 ± 0.12 | 2.03 ± 0.12 | 2.07 ± 0.13 |
| UMP | P | ARG | 166 | HH22 | 2.30 ± 0.09 | 2.29 ± 0.09 | 2.29 ± 0.10 | 2.29 ± 0.10 |
| UMP | O1P | ARG′ | 126 | HH12 | 2.14 ± 0.20 | 2.22 ± 0.19 | 2.17 ± 0.20 | 2.18 ± 0.18 |
| UMP | O1P | ARG | 21 | HE | 1.58 ± 0.09 | 1.62 ± 0.10 | 1.66 ± 0.12 | 1.69 ± 0.13 |
| UMP | O2P | ARG′ | 126 | HE | 1.70 ± 0.11 | 1.68 ± 0.11 | 1.69 ± 0.12 | 1.69 ± 0.12 |
| UMP | O2P | ARG | 166 | HH22 | 1.62 ± 0.11 | 1.66 ± 0.13 | 1.68 ± 0.14 | 1.65 ± 0.13 |
| UMP | O3P | ARG | 166 | HH12 | 1.79 ± 0.17 | 1.90 ± 0.22 | 1.9 ± 0.3 | 1.88 ± 0.22 |
| UMP | O3P | ARG | 166 | HH22 | 2.36 ± 0.17 | 2.28 ± 0.19 | 2.25 ± 0.20 | 2.29 ± 0.19 |
| UMP | O3P | ARG′ | 127 | HH11 | 1.69 ± 0.12 | 1.64 ± 0.11 | 1.64 ± 0.11 | 1.73 ± 0.15 |

Product State

| | | | | | | T/K | | |
| --- | --- | --- | --- | --- | --- | --- | --- | --- |
| | | | | | 278 | 293 | 303 | 313 |
| CYS146 | S | WAT | 40 | H2 | 1.76 ± 0.09 | 1.76 ± 0.09 | 1.77 ± 0.09 | 1.77 ± 0.09 |
| CYS146 | S | ARG | 166 | HH11 | 1.71 ± 0.08 | 1.71 ± 0.09 | 1.71 ± 0.09 | 1.71 ± 0.09 |
| UMP | O2 | ASP | 169 | H | 2.00 ± 0.13 | 2.06 ± 0.16 | 2.05 ± 0.15 | 2.01 ± 0.14 |
| UMP | P | ARG | 166 | HH22 | 2.33 ± 0.10 | 2.32 ± 0.10 | 2.33 ± 0.10 | 2.32 ± 0.10 |
| UMP | O1P | ARG′ | 126 | HH12 | 2.26 ± 0.21 | 2.33 ± 0.19 | 2.28 ± 0.19 | 2.04 ± 0.20 |
| UMP | O1P | ARG | 21 | HE | 1.58 ± 0.09 | 1.61 ± 0.10 | 1.61 ± 0.10 | 1.63 ± 0.12 |
| UMP | O2P | ARG′ | 126 | HE | 1.67 ± 0.11 | 1.65 ± 0.11 | 1.65 ± 0.11 | 1.66 ± 0.12 |
| UMP | O2P | ARG | 166 | HH22 | 1.62 ± 0.11 | 1.68 ± 0.13 | 1.68 ± 0.14 | 1.68 ± 0.13 |
| UMP | O3P | ARG | 166 | HH12 | 2.00 ± 0.18 | 2.01 ± 0.20 | 2.02 ± 0.24 | 2.12 ± 0.23 |
| UMP | O3P | ARG | 166 | HH22 | 2.37 ± 0.18 | 2.29 ± 0.19 | 2.31 ± 0.21 | 2.29 ± 0.21 |
| UMP | O3P | ARG′ | 127 | HH11 | 1.66 ± 0.11 | 1.66 ± 0.11 | 1.62 ± 0.11 | 1.62 ± 0.11 |

[a] Primed residues indicate they are from subunit B of this homodimeric protein.

with the definition of a concerted but asynchronous process. As discussed in more detail in refs 17 and 19 the temperature independence of the KIEs on this step[2] suggests that the hydride is transferred from a similar conformation at all temperatures, in accordance with the data presented in Table 1.

It is also interesting to observe how folate and UMP approach each other from reactants to transition state for the hydride to be transferred from donor to acceptor atom (see C6−C7 distance). This distance is defined as the donor−acceptor distance and its evolution is coupled with relative substrate−protein residues movements (Table 2). This coupling indicates the role of the protein dynamics in enhancing the rate of H-transfer.

From data reported in Table 2, it can be observed how a water molecule and Arg166 are both interacting with the sulfur atom of Cys146. Interestingly, the positively charged arginine serves

as a Lewis-acid that turns the thiol into a better leaving group. This arginine approaches the sulfur atom of Cys146 as the reaction proceeds, thus polarizing the electron density around the sulfur atom and stabilizing the transition state. Also, Arg166, together with Arg21, Arg126′, and Arg127′, strongly interact with phosphate oxygen atoms of dUMP. This is an interesting example of the dynamic effect that involves the protein, the reactants, and water in the active site, which would activate the C−H bond to a "tunneling ready" conformation.[2]

A complementary study to this geometrical evolution analysis is carried out by averaged substrate−protein interaction energies, calculated from reactants and transition state structures. The total average interaction potential energies over the four different temperatures are −1099.5 ± 12.5 and −1141.1 ± 5.6 kcal·mol$^{-1}$ for reactants state and transition state, respectively.

QM/MM Study of Thymidylate Synthase

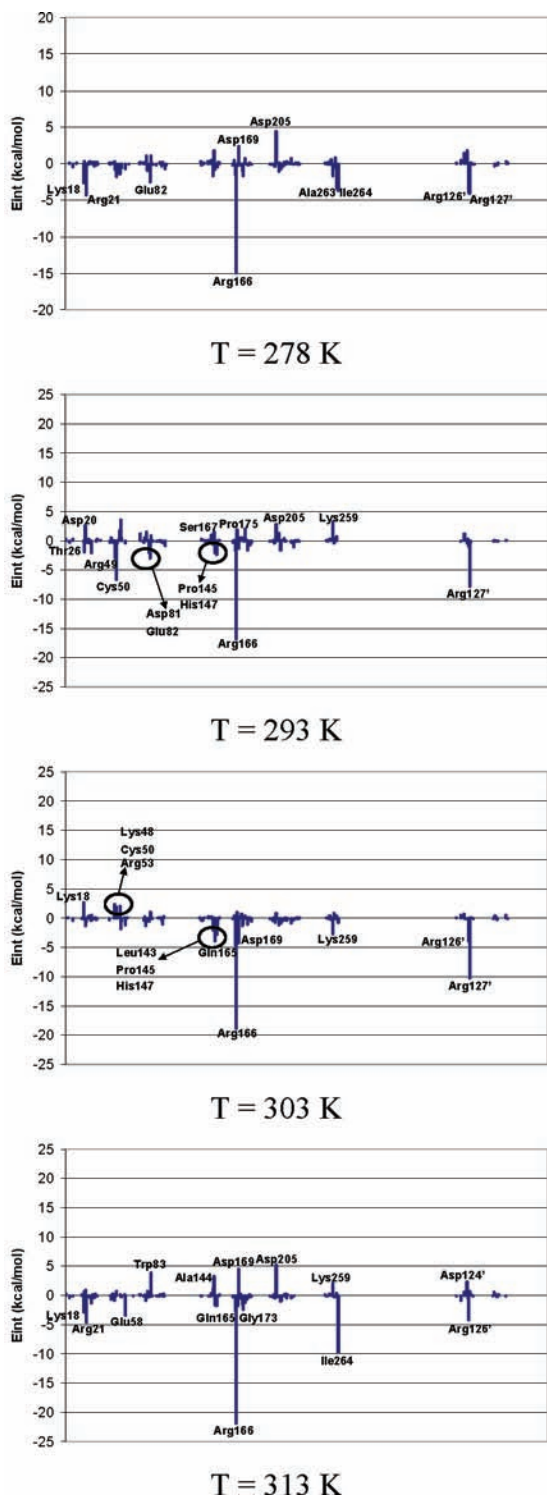*J. Phys. Chem. A, Vol. 113, No. 10, 2009* **2181**



**Figure 2.** Relative transition state stabilization, computed as averaged interaction energy differences between transition state and reactants state, by residues.

These values have no temperature dependent trend and a small standard deviation, in accordance with the observed temperature independent KIEs.[2] Additional outcome of the simulation is that, as expected from Pauling's postulate,[18] the protein interacts better with substrate in its transition state conformation than in its reactants state, which enhances confidence in the simulation procedure.

Decomposition of these substrate−protein interaction energies by residues are presented in Figure 2. In this figure, contribution of individual amino acid residues to total binding energy is presented as the difference between the transition state and reactant state. In this figure, negative values represent residues that interact better with substrate in the transition state than in the reactants state. From Figure 2 it can be observed how the preferential stabilization of transition state is achieved, at all temperatures, by means of arginine residues located around dUMP substrate: Arg21, Arg166, Arg126′, and Arg127′. It is important to point out that the patterns of interactions established between substrate and protein, and cofactor and protein are very similar at all temperatures, both at the reactant state and at the transition state, as revealed not only by data reported in Table 1 and 2 but also by analysis of interaction energies by residue carried out at the two states (see Supporting Information). Nevertheless, from Figure 2, where differences of interaction energies between both states are plotted, it can be observed that Arg166 preferentially stabilizes the transition state at all temperatures. This energetic contribution of Arg166 to the stabilization of the transition state reflects its role in activating the cleavage of the thioether bond (C−S) and further supports the concerted nature of this cleavage and the hydride transfer form C6 of the $H_4$folate to the exocyclic methylene of the intermediate (step 5 in Scheme 2).

## Conclusions

A theoretical study of the reduction of exocyclic methylene intermediate by hydride transfer from the 6S position of $H_4$ folate, which is the rate-limiting step of the TS catalyzed reaction, has been carried out using hybrid QM/MM methods. We have examined this step in terms of free energy surfaces obtained at four different temperatures: 273, 293, 303, and 313 K. The high similarity of the PMFs in all temperatures is in good agreement with the temperature independent KIEs measured at the same temperatures.[2] A significant outcome of these calculations addresses a long lasting open question in the TS catalysis: is the tunneling of the hydride from $H_4$ folate to the covalently bound intermediate, and does the dissociation of the enzymatic thiol from the C6 carbon of dTMP constitutes a stepwise addition elimination reaction or a concerted 1,3-$S_N$2 substitution? The calculations indicate that the hydride transfer and the scission of the conserved active site cysteine residue (Cys146 in *E. coli*) take place in a concerted but asynchronous way, assisted by residues in the active site that polarize the carbon−sulfur bond and stabilize the charge transferred from cofactor to substrate. Between these residues, Arg166 seems to play a significant role in stabilizing the transition state.

Finally, the role of enzyme dynamics in activating a specific chemical step in its catalyzed reaction has been a matter of great interest in contemporary enzymology. In ref 2 we measured intrinsic KIEs on the same H-transfer step. These experimental KIEs were temperature independent and the Marcus-like model was used to suggest that such a phenomenon indicates H-tunneling from an ideal donor−acceptor distance and well-tuned reorganization of the reaction coordinate throughout the experimental temperature range.[17,18] The current simulation indicates that the effective transition state for this reaction is indeed temperature independent and critically identifies the atomic and molecular dynamics that constitute the reorganization term in the Marcus-like model used in ref 2. This motion of the protein toward the transition state and the electronic and geometrical details of that state are of critical importance in inhibitors and drug design.[20] Moreover, although we did not calculate rates or KIEs, the calculated transition state geometry is relevant to small curvature tunneling (SCT) and the PMF landscape close to the transition state is relevant to large curvature tunneling

(LCT).[21] In the context of the current work, it is of critical importance that these features of our PMFs are temperature independent, because this dictates temperature independent KIEs regardless of the method used to calculate reaction rates or KIEs.

Consequently, we believe that the current study may enhance rational design of potent and specific inhibitors as leads toward new antibiotic and chemotherapeutic drugs.

**Supporting Information Available:** Interaction energies between substrate−protein and cofactor−protein, computed by residue, at the reactants state and the transition state at the four temperatures are presented in Figure S1. This material is available free of charge via the Internet at http://pubs.acs.org.

### References and Notes

(1) Kanaan, N.; Martí, S.; Moliner, V.; Kohen, A. *Biochemistry* **2007**, *46*, 3704–3713.
(2) Agrawal, N.; Hong, B.; Mihai, C.; Kohen, A. *Biochemistry* **2004**, *43*, 1998–2006.
(3) Carreras, C. W.; Santi, D. V. *Annu. Rev. Biochem.* **1995**, *64*, 721–762.
(4) Montfort, W. R.; Perry, K. M.; Fauman, E. B.; Finer-Moore, J. S.; Maley, G. F.; Hardy, L.; Maley, F.; Stroud, R. M *Biochemistry* **1990**, *29*, 6964–6977.
(5) Finer-Moore, J. S.; Montfort, W. R.; Stroud, R. M. *Biochemistry* **1990**, *29*, 6977–86.
(6) Perry, K. M.; Fauman, E. B.; Finer-Moore, J. S.; Montfort, W. R.; Maley, G. F.; Maley, F.; Stroud, R. M. *Proteins: Struct., Funct. Genet.* **1990**, *8*, 315–333.
(7) Field, M. J. *A practical introduction to the simulation of molecular systems*; Cambridge University Press: Cambridge, U.K., 1999.
(8) Antosiewicz, J.; McCammon, J. A.; Gilson, M. K. *J. Mol. Biol.* **1994**, *238*, 415–436.
(9) Field, M.; David, L.; Rinaldo, D. Personal communication, 2006.
(10) Dewar, M. J. S.; Zoebisch, E. G.; Healy, E. F.; Stewart, J. J. P. *J. Am. Chem. Soc.* **1985**, *107*, 3902–3909.
(11) Kaminiski, G. A.; Friesner, R. A.; Tirado-Rives, J.; Jorgensen, W. L. *J. Phys. Chem. B* **2001**, *105*, 6474–6487.
(12) Jorgensen, W. L.; Chandrasekhar, J.; Madura, J. D.; Impey, R. W.; Klein, M. L. *J. Chem. Phys.* **1983**, *79*, 926–935.
(13) Warshel, A.; Levitt, M. *J. Mol. Biol.* **1976**, *103*, 227–249.
(14) Singh, U. C.; Kollman, P. A.; Karplus, M. *J. Comput. Chem.* **1986**, *7*, 718–730.
(15) Kumar, S.; Bouzida, D.; Swendsen, R. H.; Kollman, P. A.; Rosenberg, J. M. *J. Comput. Chem.* **1992**, *13*, 1011–1021.
(16) Torrie, G. M.; Valleau, J. P. *J. Comput. Phys.* **1977**, *23*, 187–199.
(17) Kohen, A. Kinetic isotope effects as probes for hydrogen tunneling in enzyme catalysis. In *Isotope Effects in Chemistry and Biology*; Kohen, A., Limbach, H. H., Eds.; Taylor & Francis-CRC Press: Boca Raton, FL, 2006; Chapter *28*, pp 743−764.
(18) Pauling, L. *Chem. Eng. News* **1946**, *24*, 1375–1377.
(19) Nagel, Z. D.; Klinman, J. P. *Chem. Rev.* **2006**, *106*, 3095–3118.
(20) Taylor Ringia, E. A.; Tyler, P. C.; Evans, G. B.; Furneaux, R. H.; Murkin, A. S.; Schramm, V. L. *J. Am. Chem. Soc.* **2006**, *128*, 7126–7127.
(21) Gao, J.; Ma, S.; Major, D. T.; Nam, K.; Pu, J.; Truhlar, D. G. *Chem. Rev.* **2006**, *106*, 3188–3209.

JP810548D